AERODYNAMIC LOAD COMPONENTS EVALUATION OF THE TWO-STAGE SOUNDING ROCKET VEHICLE SONDA III

Maria Luísa Collucci da Costa Reis, marialuisamlccr@iae.cta.br, 55 12 3947-6503
João Batista Pessoa Falcão Filho, jb.falcao@ig.com.br, 55 12 3947-6498
Instituto de Aeronática e Espaço, Praça Mal. Eduardo Gomes, 50, CEP 12226-904

Roberto da Mota Girardi, girardi@ita.cta.br, 3947-5976
Instituto Tecnlógico de Aeronáutica, Praça Mal. Eduardo Gomes, 50, CEP 12228-900

Abstract. *Model of aerospace vehicles are tested in wind tunnels in order to predict their perfomance in real flight situations. Data originating from wind tunnel tests are used for the optimization of aerodynamic projects. The purpose of this study is to analyse the aerodynamic load coefficients of the Brazilian sounding rocket Sonda III, developed by the Institute of Aeronautics and Space. A campaign is in progress to test several configurations of the vehicle in the subsonic and transonic regime of airflow. The aerodynamic facility used to carry out the tests is the Pilot Transonic Wind Tunnel, located at the Aerodynamic Division of the Institute. The results presented in this paper include the drag force, side force and lift force coefficients and the pitching, rolling and yawing moment coefficients. The test article considered is the bi-stage model, composed of the first and the second stage of the vehicle. An internal multi-component balance is employed to supply the force and moment readings. It measures the loads by using strain gauges arranged in Wheatstone bridges. The internal balance is fitted into the model being tested. Besides the aerodynamic components, the measured parameters include total pressure and static pressure of the airflow. The static pressure sensor is positioned at the inlet of the wind tunnel test section and the total pressure sensor is located at the stilling chamber of the circuit. The instrumentation is calibrated prior to the tests and the uncertainties in the quantities involved are estimated according to international standardization. Data reduction supplies load coefficient curves for angles of attack ranging from -10 ^{o} to +10 ^{o} for Mach number regimes varying from 0.3 to 1.0. Source of errors presented in the measurements are also analysed and quantified, and the procedures adopted to minimize them are reported in this paper. Their contribution to the final uncertainty is considered by applying the law of propagation of uncertainty to the coefficient quantities. Experimental data originating from these wind tunnel tests can be compared to theoretical results and can contribute to the optimization of vehicles developed by Brazilian space programs.*

Keywords*: sounding rocket vehicles, transonic wind tunnels, metrological reliability*

1. INTRODUCTION

The vehicle SONDA III (Fig. 1) is a sounding rocket developed by the Brazilian Institute of Aeronautics and Space (IAE). This is a two stage vehicle with a 30 cm diameter second stage, capable of carrying a payload of approximately 100 kg up to an altitude of 600 km. It is one of the sounding rocket family named Sonda, which started with Sonda I, first launched in 1965.

Figure 1. The Sonda III bi-stage suborbital vehicle.

The Sonda family has been used in scientific missions, to investigate the behavior of biological, chemical and physical systems under weightless conditions and in the development of Global Positioning Satellite (GPS) technology for space applications.

Experimental tests of several Sonda III model configurations have recently been carried out in the Pilot Transonic Wind Tunnel of the Institute of Aeronautics and Space (Fig. 2). In a wind tunnel, the air flows over the test article, simulating actual flight conditions. The data originating from the wind tunnel tests is important for the prediction of a vehicle's flight performance and can be compared to available theoretical simulation data.

Figure 2. The Pilot Transonic facility.

This paper presents the aerodynamic forces and moments coefficients of the complete vehicle, composed of the first and the second stage. The quality of data is also addressed by estimating the uncertainties in the coefficients. The methodology employed for the assessment of uncertainty is that recommended by the Member States of the Metre Convention (ISO/BIPM, 1995).

The procedures and methodologies employed will be used as a guide in future tests for other aerospace vehicles developed by Brazilian aerospace programs.

2. THE WIND TUNNEL TEST

The Pilot Transonic wind tunnel is one of a closed circuit kind, where the airflow is not in contact with atmosphere. It operates continuously when driven by an axial compressor (also called main compressor). A schematic picture of the aerodynamic circuit is presented in Figure 3, highlighting its main parts: the axial compressor, cooler, stilling chamber, plenum chamber, high velocity diffuser and corners (numbered from 1 to 4). Arrows indicate the direction of the airflow. The test section, which receives the test article, is located in the plenum chamber (Falcão Filho and Mello, 2002).
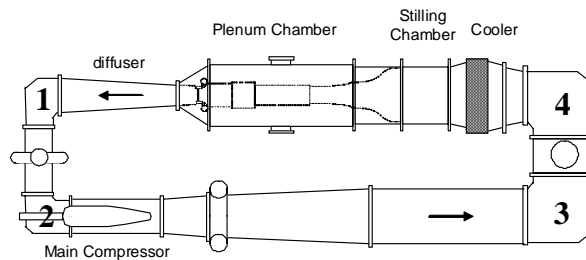
Figure 3. Schematic picture of the wind tunnel circuit.

A sting support was used to fix the bi-stage model. The fins of the model were aligned in a crossed position (⊕) in relation to the wind tunnel test section (Fig. 4).

Figure 4. Model inside the test section.

The model is 395 mm long and has a mass of approximately 300 g. The centre of gravity is located at 143,2 mm from the aft to the forward part of the fuselage.

An internal multi-component balance is used to measure the aerodynamic loads (Figure 5). It is designed to fit within the model under test and is connected to the sting support (Figure 6). Strain-gages arranged in Wheatstone bridges supply the readings.

A calibration is carried out prior to the tests. It is very important to recognize and minimize the source of errors presented in the balance calibration because it represents the dominant contribution to the overall uncertainty in wind tunnel testing (AIAA, 2003).
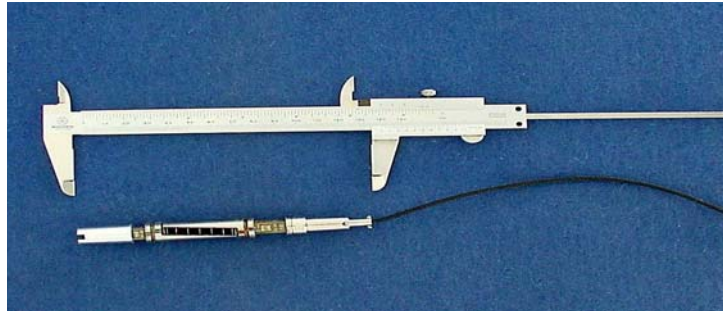
Figure 5. Internal aerodynamic balance.
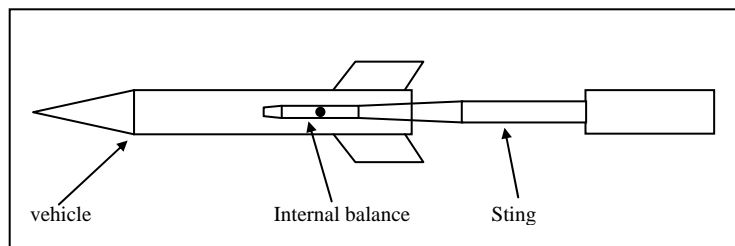
Figure 6. Schematic picture of the model-internal balance-sting assembly.

Sonda III was tested in subsonic and transonic regimes, at nominal Mach numbers M varying from 0.30 to 1.00, for angles of attack α varying from -10° up to +10°, 2° stepwise.

3. DATA REDUCTION

3.1. Aerodynamic forces and moments

In this paper, the terminology employed for designating aerodynamic loads is: drag force (D), side force (SF), lift force (L), rolling moment (r), pitching moment (m) and yawing moment (y).

The force coefficients, C_F, and the moment coefficients, C_M, are evaluated through the expressions (1) and (2) respectively:

$$C_F = \frac{Force}{qA} \qquad (1)$$

$$C_M = \frac{Moment}{qAl} \qquad (2)$$

Force: aerodynamic force (drag, side or lift);
Moment: aerodynamic moment (rolling, pitching or yawing);
q: dynamic pressure;
A: reference area; and
l: reference length.

The reference area used, A, which corresponds to the cross sectional area of the fuselage of the model, is equal to 6.2×10^{-4} m^2. The reference length, l, corresponds to the diameter of the first stage, and it is equal to 2.8×10^{-2} m.

3.2. Law of propagation of uncertainty

According to ISO/BIPM (1995), the value of the uncertainty in measurement is the positive root square of Eq. (3):

$$u_c^2 = \sum_{i=1}^{N} \left(\frac{\partial y}{\partial x_i} \right)^2 u^2(x_i) \tag{3}$$

where y is the output quantity and $x_{i's}$ are the input quantity. Equation (3) is called the law of propagation of uncertainty.

Applying Eq. (3) to Eqs. (1) and (2) results in the values of the uncertainty in the aerodynamic load coefficients. For example, for the drag force coefficient, C_D, the estimated uncertainty is:

$$u_{C_D}^2 = \left(\frac{\partial C_D}{\partial D} \right)^2 u_D^2 + \left(\frac{\partial C_D}{\partial q} \right)^2 u_q^2 + \left(\frac{\partial C_D}{\partial A} \right)^2 u_A^2 \tag{4}$$

which leads to:

$$u_{C_D}^2 = \left(\frac{1}{qA} \right)^2 u_D^2 + \left(\frac{-D}{q^2 A} \right)^2 u_q^2 + \left(\frac{-D}{qA^2} \right)^2 u_A^2 \tag{5}$$

The same procedure is applied to side force, C_{SF}, lift force, C_L, pitching moment, C_m, rolling moment, C_r, and yawing moment, C_y.

3.3. Dynamic pressure and Mach number

Equations (6) and (7) are used to evaluate the Mach number M and the dynamic pressure q of the flow, respectively (Anderson, 1985).

$$M^2 = \frac{2}{\gamma - 1} \left[\left(\frac{p_0}{p} \right)^{\frac{(\gamma - 1)}{\gamma}} - 1 \right] \tag{6}$$

$$q = \frac{\gamma}{2} p_0 \frac{M^2}{\left(1 - \frac{\gamma - 1}{2} M^2 \right)^{\frac{\gamma}{\gamma - 1}}} \tag{7}$$

where p_0 is the total pressure, p is the static pressure and $\gamma = c_p/c_v$, is the ratio of specific heat, equal to 1.4 for air.

The static pressure sensor is positioned on the upper part of the wall at the beginning of the wind tunnel test section and the total pressure sensor is located in the stilling chamber of the circuit.

4. RESULTS AND DISCUSSION

4.1. Drag force coefficient

Figure 7 presents the drag coefficient, C_D, versus angle of attack α, for Mach number $M = 0.30$. Near $\alpha = 0^o$, the behavior of this aerodynamic load component is as predicted (Schlichting, 1979). The drag coefficient is approximately proportional to the square of the angle of attack α. The 95% uncertainty limits are presented as well (ISO/BIPM, 1995).

Verifying the measurement precision of the input quantities in Eqs. (1) and (2) has shown that the uncertainties in forces and moments are the most important components for the uncertainty in the aerodynamic coefficients.

For example, considering the drag force, the term u_D in Eq. (5) is the dominant component in the uncertainty of the drag coefficient, u_{CD}, being the other terms, u_q and u_A, negligible. Two sources of errors contribute to the uncertainty u_D: the balance calibration and the variation of the wind tunnel airflow. The variation in the signal is quantified through the standard deviation.

Although it is expected a dispersion in the model attitude caused by instabilities in the flow during the tests, no uncertainty is attributed to α, due to difficulties in assessing it.

Drag coefficient and uncertainty limits versus angle of attack
M = 0.30
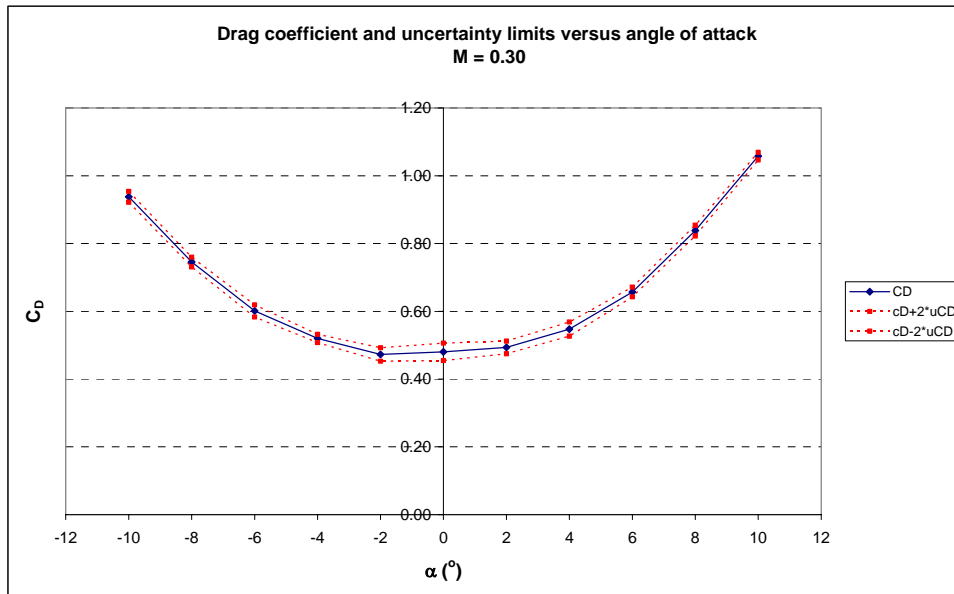
Figure 7. C_D versus α and uncertainty limits.

One can see that the curve in Fig. 7 is not symmetrical in relation to the axis corresponding to the angle of attack equal to zero. The lack of symmetry may be caused by the presence of the support system of the model, whose structure protrudes into the flow thereby increasing the blockage for negative angles of attack.

In order to compare the uncertainties of all the six aerodynamic coefficients, their corresponding values are shown in Tab. 1 for $\alpha = 0^o$ and $M = 0.30$. It can be seen that the lift and the side forces have the highest ones. This behavior has also been observed in previous tests (Reis, 2010) and reflects the errors of readings of the strain-gages related to these components. A quantification of the aerodynamic loads uncertainties in the calibration process is described in (Reis, 2008).

Table 1. Uncertainty values in the aerodynamic coefficients. $M = 0.30$.

α (°)	Forces ($\times 10^{-2}$)			Moments ($\times 10^{-2}$)		
	u_{CD}	u_{CSF}	u_{CL}	u_{Cr}	u_{Cm}	u_{Cy}
0	1.3	4.6	7.5	0.3	0.2	0.2

An error in the test methodology was recognized in the campaign of the two-stage vehicle, corresponding to the model's weight P. The weight component $mgsen\alpha$, parallel to the longitudinal axis of the fuselage, influences the drag force. (Fig. 8).
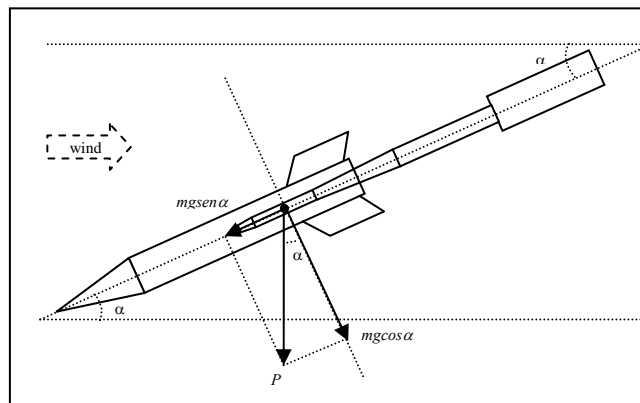
Figure 8. Influence of model's weight P on the aerodynamic load reading.

To correct this influence, prior to the tests, balance reading acquisition must be carried out with no wind, for each angle of attack. The balance calibration process results in positive drag forces for a positive axis system relative to the wind direction. Without wind, the balance sensors give a negative drag value for negative angles of attack. For $\alpha > 0$, the readings are positive. The corrected drag force is obtained subtracting the readings acquired during the test by the previous ones obtained when the tunnel is turned off. In Fig. 9 one can compare both curves for the corrected and uncorrected drag coefficient.

A similar procedure is adopted for the lifting and pitching coefficients, due to the perpendicular weight component.
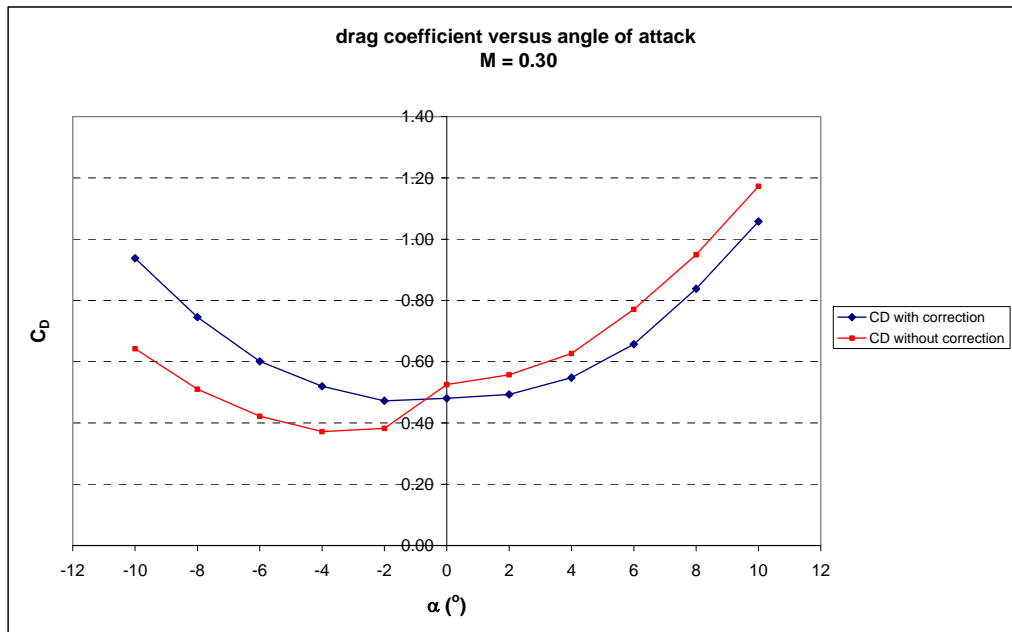
Figure 9. Correction of drag coefficient due to the model weight.

Figure 10 shows curves $C_D \times \alpha$ for the range of Mach numbers covered in the tests. Uncertainty limits were suppressed for clarity. One notices that the curve $M = 1.00$ is distant from the general tendency presented by the others, as predicted in literature. This behavior can be seen in Fig. 11 as well, with an increase in the C_D value for $\alpha = 0^o$ in the region of Mach number equal to 1.00.
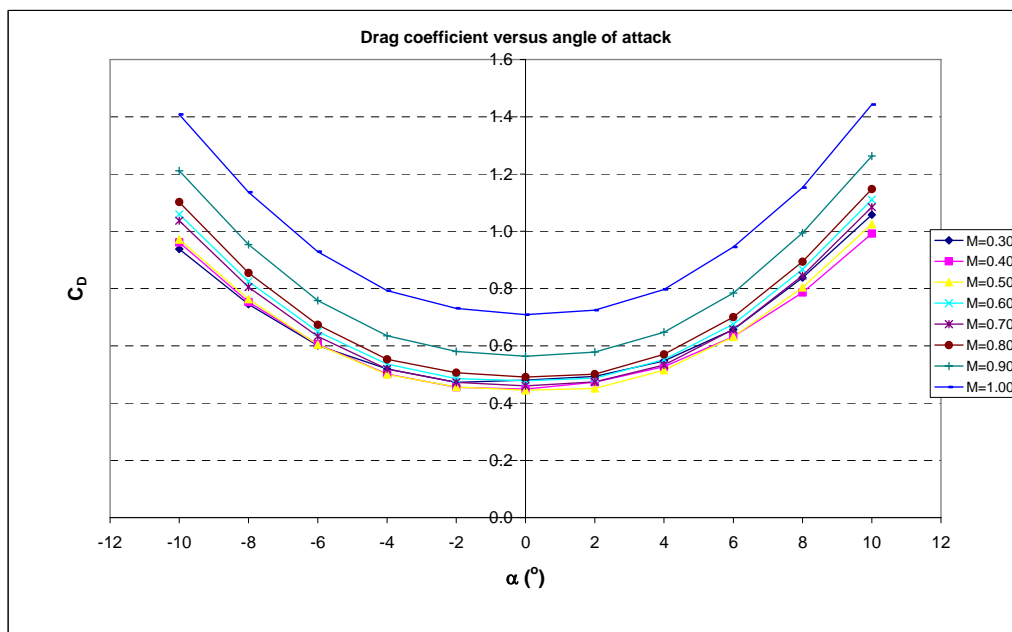
Figure 10. $C_D \times \alpha$ family curves.
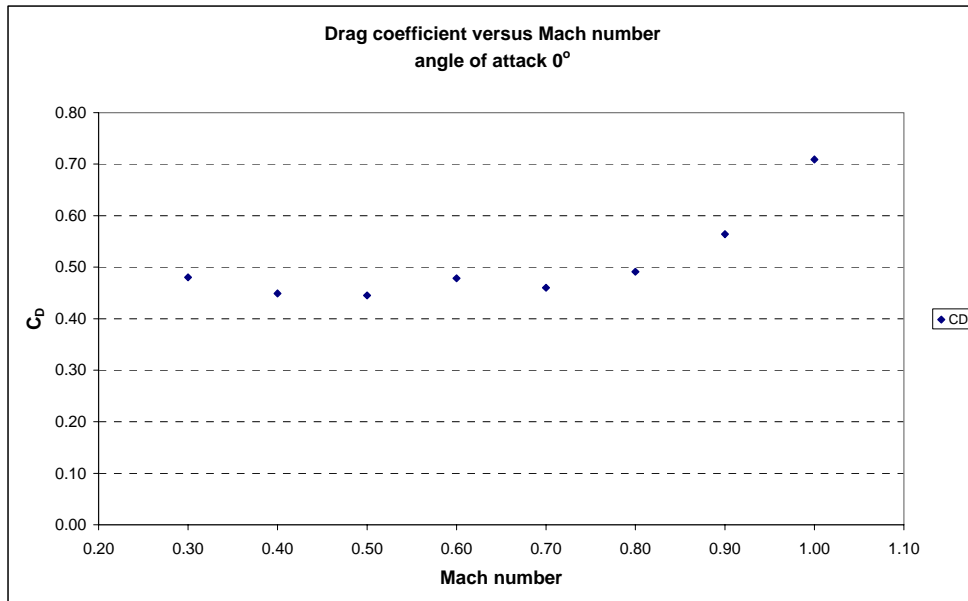
Figure 11. The dependence of C_D on Mach number.

4.2. Lift force coefficient

Variations of lift force coefficient C_L with angle of attack are presented in Fig. 12, for several Mach numbers. Lift coefficient increases when the attitude α of the vehicle increases. An error occurred in the C_L value for $M = 0.30$ at angle of attack null. It was expected to be equal to zero. The reason for this discrepancy is under investigation.
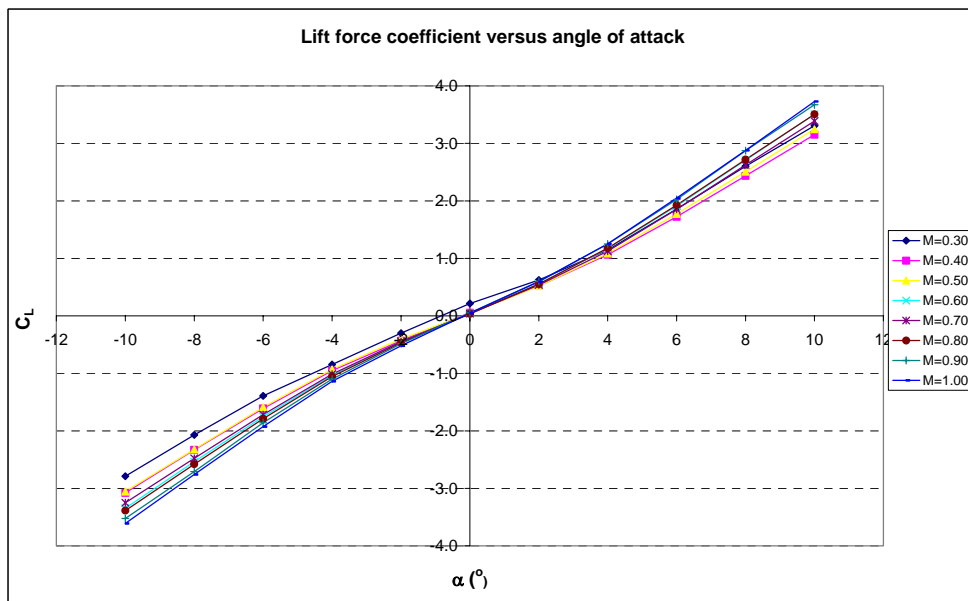
Figure 12. Variation of lift force coefficient with Mach number.

4.3. Pitching moment coefficient

The family curves $C_m \times \alpha$ for several Mach numbers are presented in Fig. 13. The pitching moment decreases for rising values of α.
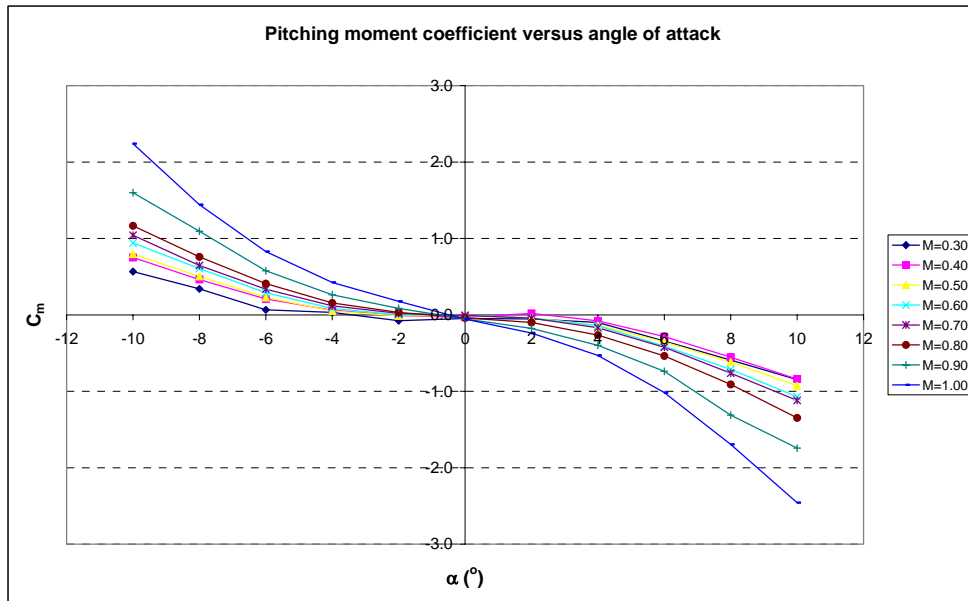
Figure 13. Curves $C_m \times \alpha$.

4.4. Side force coefficient

As there is no side slip angle in this test campaign, no side force is expected in the tests. They should be equal to zero for all the range of angles of attack considered. Care must be taken when aligning the model in relation to the axis of the wind tunnel test section to avoid spurious effects. Figure 14 present curves $C_{SF} \times \alpha$. Comparing the scale of the y-axis of Fig. 14 with Figs. 10, 12 and 13, we can notice that the values of the side force coefficients are ten times lower than the other components and are inside the uncertainty limits of the measurement.
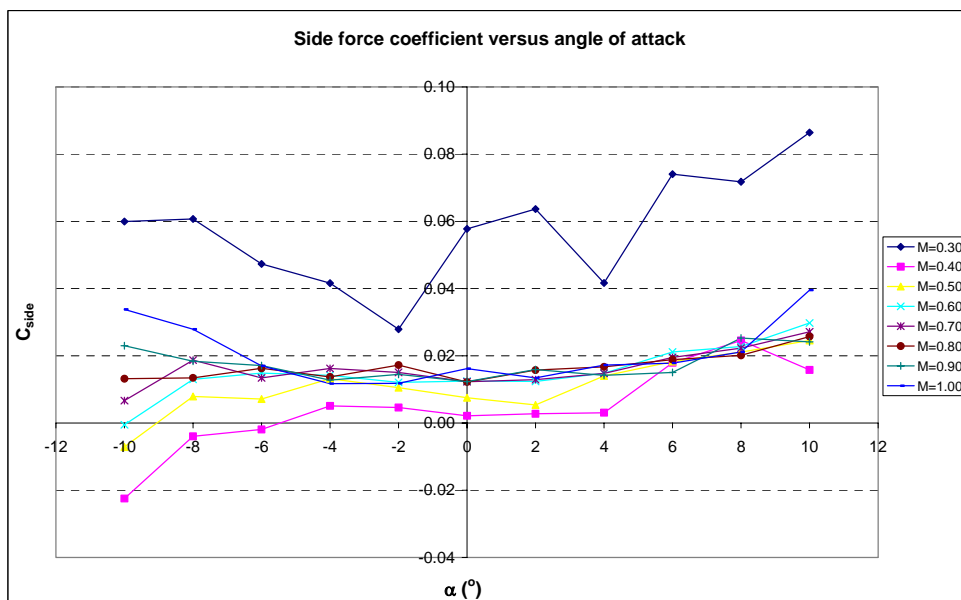
Figure 14. Side force coefficient versus angle of attack.

4.5. Yawing moment coefficient

Curves $C_y \times \alpha$ are presented in Figure 15. Their magnitudes are expected to be low for the same reasons as discussed in the case for the side force coefficient.
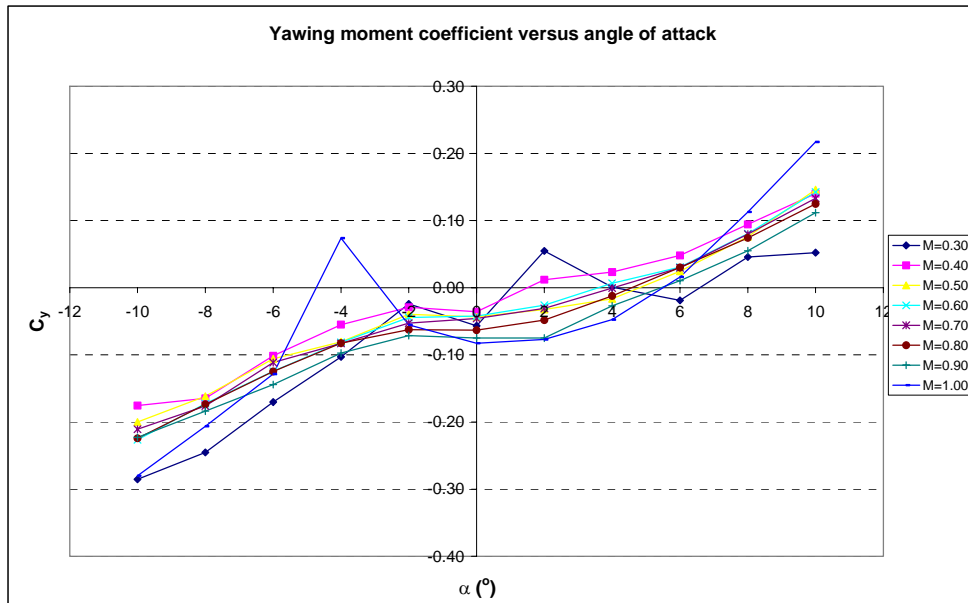
Figure 15. Yawing moment coefficient curves.

4.6. Rolling moment coefficient

For the model configuration with fins aligned at 0° to the axis of fuselage, the rolling moment coefficients values must be around zero value. Curves $C_r \times \alpha$ are presented in Figure 16.
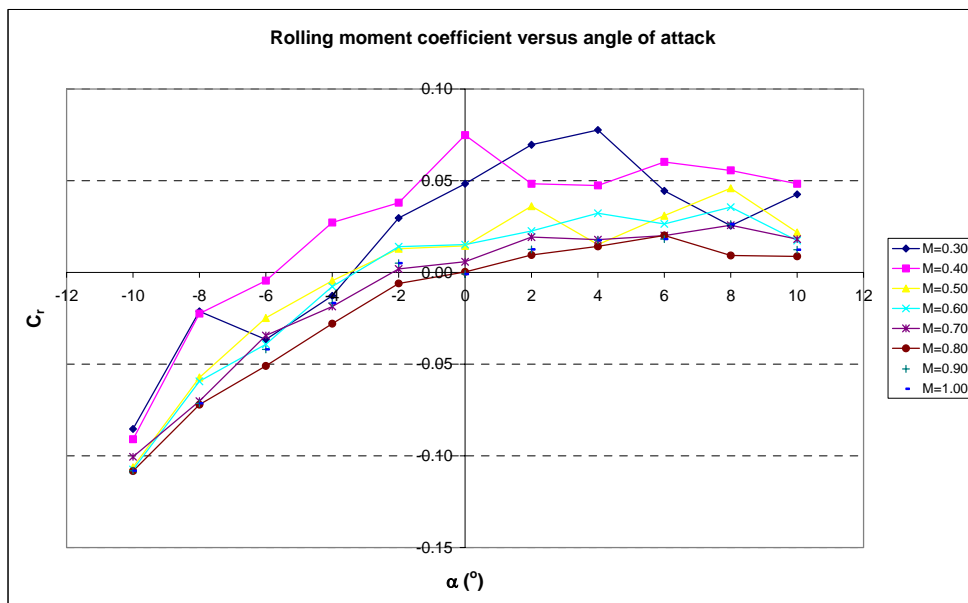
Figure 16. Curves $C_r \times \alpha$.

5. CONCLUSIONS

The values of the drag, side and lift force coefficients and the rolling, pitching and yawing moment coefficients of the bi-stage vehicle Sonda III were estimated. The behavior of the data in the subsonic and transonic regimes is compatible with that reported in specialized literature.

The contribution of the errors in the measured parameters was considered by employing standard methodology for the assessment of uncertainty in the aerodynamic coefficients.

Recognized source of errors were analyzed and their influence quantified. Some of them have not been solved yet, as the unexpected value of C_L at $\alpha = 0^o$, for $M = 0.30$. The causes are under investigation.

6. REFERENCES

AIAA, 2003, R-091-2003 Recommended Practice,"Calibration and Use of Internal Strain-Gage Balances with Application to Wind Tunnel Testing", American Institute of Aeronautics and Astronautics, VA, USA, 64 p.

Anderson Jr., J. D., 1985, "Introduction to Flight", McGraw-Hill, 3th edition, 616 p.

Falcão Filho, J. B. P., Mello, O. A. F., 2002, "Technical Description of the CTA's Pilot Transonic Wind Tunnel", IX Brazilian Thermal Engineering and Sciences, Caxambu, MG, Brazil.

ISO/BIPM, 1995, "Guide to the Expression of Uncertainty in Measurements", 101 p.

Reis, M. L. C. C., Castro, R. M., Falcão Filho, J. B. P., Barbosa, I. M., Mello, O. A. F., 2008, "Calibration Uncertainty Estimation for Internal Aerodynamic Balance", XII IMEKO TC1&TC7 Joint Symposium, Annecy, France.

Reis, M. L. C. C., Falcão Filho, J., Mello, O. A. F., 2010, "Wind Tunnel Tests of the Sonda III Space Vehicle", VI National Congress of Mechanical Engineering, Campina Grande, PB, Brasil.

Schlichting, H., Truckenbrodt, E., Ramm, H. J., 1979, "Aerodynamics of the Airplane", McGraw-Hill, 541 p.

7. RESPONSIBILITY NOTICE

The authors Reis, Falcão Filho and Girardi are the only persons responsible for the printed material included in this paper.